

Article

Relative Energetics at the Semiconductor/Sensitizing Dye/Electrolyte Interface

Arie Zaban, Suzanne Ferrere, and Brian A. Gregg

J. Phys. Chem. B, **1998**, 102 (2), 452-460 • DOI: 10.1021/jp972924n

Downloaded from <http://pubs.acs.org> on December 4, 2008

More About This Article

Additional resources and features associated with this article are available within the HTML version:

- Supporting Information
- Links to the 9 articles that cite this article, as of the time of this article download
- Access to high resolution figures
- Links to articles and content related to this article
- Copyright permission to reproduce figures and/or text from this article

[View the Full Text HTML](#)



ACS Publications
High quality. High impact.

Relative Energetics at the Semiconductor/Sensitizing Dye/Electrolyte Interface

Arie Zaban,^{*,†} Suzanne Ferrere, and Brian A. Gregg*

National Renewable Energy Laboratory, 1617 Cole Boulevard, Golden, Colorado 80401-3393

Received: September 8, 1997; In Final Form: November 6, 1997

Chemical oxidation, spectro-electrochemical reduction, and potential-dependent photoluminescence were employed to investigate changes in the redox potential of eight different adsorbed sensitizing dyes relative to the potentials of the semiconductor and the electrolyte solution. The redox potentials of the investigated dyes were pH-independent in solution but developed a pH dependence that varied between 21 and 53 mV per pH unit upon adsorption to an oxide surface. Electrochemical experiments show that the apparent redox potential of the dye could also be influenced by an external bias applied to the electrode. The adsorption-induced potential changes were found to depend on both the dye structure and the electrolyte composition. A proposed model that considers the position of the specifically adsorbed dye relative to the ionic double layer at the electrode/electrolyte interface explains these results qualitatively. When the dye is mostly inside the double layer, its potential will tend to follow changes in the semiconductor potential; when it is mostly outside, its potential will be almost independent of the semiconductor. The fact that the potential of the sensitizing dye is not fixed relative to either the semiconductor or the electrolyte solution has important implications for the understanding and optimization of dye-sensitized cells.

Introduction

Sensitization of wide band gap semiconductors with organic and inorganic dyes is currently of great interest in solar energy conversion systems.¹ Dye-sensitized solar cells that convert light to electrical energy at efficiencies as high as 10%,^{2,3} and other applications like self-powered electrochromic windows⁴ and light-emitting diodes⁵ have been reported. Studies concerning the fundamental understanding of the dye-TiO₂ system^{6–10} and new materials like other high surface area semiconductors^{11,12} and new sensitizers^{13–16} have appeared recently. The increasing research effort toward higher efficiencies and solid-state versions of these cells^{17–21} is evident from the literature.

The dye-sensitization process is based on charge separation at the semiconductor/dye/electrolyte interface.²² Fast electron injection from the dye to the semiconductor occurs upon illumination followed by hole transfer to the electrolyte solution (regeneration of the dye).^{22–24} Many factors, such as the distance between the dye and the semiconductor,²⁵ the type of bond that connects them^{26,27} and the properties of the redox couple in the electrolyte solution,²⁸ influence the efficiency of the process.

Perhaps the most fundamental property that should be considered during the design of such cells is the relative energies at the semiconductor/dye/electrolyte interface. The dye excited-state oxidation potential has to be more negative than the semiconductor conduction band potential to enable the electron injection, and the oxidation potential of the dye must be more positive than the redox couple in the electrolyte solution to provide the driving force for the hole transfer.^{22,29} Within these limits, the cell performance is affected by the exact position of the relative potentials. A change in either of the two driving forces impacts both the short circuit photocurrent and the open circuit photovoltage of the cell.^{22,30} Therefore, optimization of

the dye-sensitized solar cells must involve considerations regarding the semiconductor, dye, and electrolyte energetics.²⁹

All four potentials that affect the semiconductor/dye/electrolyte interface can be measured separately: the conduction band potential of the high surface area semiconductor can be resolved by measurements of its absorption³¹ or reflection³² during a potential sweep, the oxidation potential of the dye in solution and the potential of the redox couple can be measured by cyclic voltammetry,³³ and the dye's excited-state potential can be estimated from its oxidation potential and the excited-state energy.^{13,22} However, measurements of these potentials under working cell conditions, i.e., when the dye is adsorbed onto the semiconductor and the electrolyte solution is present, are more complicated. The complexity arises mostly from the limited electrochemical window resulting from the insulating nature of the TiO₂ at positive bias³⁴ and the tendency of the dye to desorb at negative bias.⁶ It is, therefore, usually assumed that the potentials measured individually still pertain when the complete solar cell is assembled.

In a previous paper³⁵ we reported measurements of the redox potential of one ruthenium-based dye adsorbed on TiO₂ as a function of solution pH. The redox potential was determined by chemical oxidation with aqueous bromine solution. We found that, upon adsorption onto the TiO₂, the redox potential of the dye became pH-dependent, changing by 53 mV per pH unit, although the potential of the dye in solution was independent of pH. The pH sensitivity of the redox potential induced by adsorption onto TiO₂ was assumed to be correlated to the well-known movement of the TiO₂ conduction band by 59 mV per pH unit.^{36,37} However, at that point we were unable to provide a definitive mechanism for this process.

In this paper, a more comprehensive study of the effect of adsorption on the redox potential of the dye is reported. The redox potential was investigated by chemical oxidation, spectro-electrochemical reduction, and potential dependent photoluminescence. Five ruthenium dyes, two phthalocyanine dyes, and

[†] Current address: Department of Chemistry, Bar-Ilan University, Ramat Gan 52900, Israel.

a perylene dye were investigated. The six dyes tested for pH dependence exhibited a pH-dependent redox potential induced by adsorption to TiO₂ or to insulating Al₂O₃. The magnitude of the pH sensitivity varied between 21 and 53 mV per pH unit depending on the dye structure. Electrochemical experiments showed that the redox potential of the dye was also affected by an externally applied bias. This sensitivity to pH and electrical bias depends both on the ability of electrolyte ions to penetrate the dye layer and on the dye structure. The crucial parameter is the position of the specifically adsorbed dye relative to the ionic double layer (Helmholtz and diffuse layers). The mechanism by which the adsorption affects the redox potential, and the importance of these findings to the design and understanding of dye-sensitized systems, will be discussed.

Experimental

Materials and Methods. 2,2'-bipyridine, 4,4'-dimethyl-2,2'-bipyridine, 3,4,9,10-perylenetetracarboxylic acid dianhydride, and RuCl₃·3H₂O were obtained from Aldrich. 4,4'-Dicarboxylic acid-2,2'-bipyridine was obtained from Alfa/Aesar. All other synthetic starting materials were reagent or ACS grade.

Preparation of Pyridyl Ligands. 1,2-bis[4'-methyl-2,2'-bipyridyl-4-yl]ethane,³⁸ 4,4'-bis(bromomethyl)-2,2'-bipyridine,³⁹ and 4-bromo-2,2'-bipyridine⁴⁰ were prepared via published procedures. 4,4'-Bis(diethyl methylphosphonate)-2,2'-bipyridine was prepared from 4,4'-bis(bromomethyl)-2,2'-bipyridine according to a method used by Hupp⁴¹ and chromatographed on silica gel using 10% acetone in dichloromethane as eluent. 4-Bromo-2,2'-bipyridine was converted to 4-diethyl phosphonate-2,2'-bipyridine using the procedure of Hirao et al.⁴² 4,4',5,5'-Tetramethyl-2,2'-bipyridine was a gift of Professor C. Michael Elliott, prepared from 3,4-lutidine.⁴³ 4'-Diethyl phosphonate-2,2':6',2''-terpyridine was prepared via the same three-step sequence employed by Grätzel.^{42,44,45}

[Ru^{II}(4'-phosphonic acid-2,2':6',2''-terpyridine)(1,2-bis[4'-methyl-2,2'-bipyridyl-4-yl]ethane)(CN)] (Dye 1). [Ru(4'-diethyl phosphonate-2,2':6',2''-terpyridine)(Cl)₃] was prepared via a modification of a literature procedure.⁴⁶ In a typical preparation, 800 mg of RuCl₃·3H₂O (3.07 mmol) was dissolved in 175 mL of absolute ethanol and degassed with N₂. To the solution was added 1.13 g (3.05 mmol) of 4'-diethyl phosphonate-2,2':6',2''-terpyridine, and the reaction mixture refluxed for 5 h under N₂. The brown solution was allowed to cool to room temperature and the resulting copper-colored precipitate was collected by vacuum filtration. The product was rinsed with 3 × 25 mL portions of ethanol and dried under vacuum. A typical yield was 1.3 g (74%). Subsequently, [Ru(4'-diethyl phosphonate-2,2':6',2''-terpyridine)(1,2-bis[4'-methyl-2,2'-bipyridyl-4-yl]ethane)(Cl)] was prepared by reaction of 3.0 g of [1,2-bis[4'-methyl-2,2'-bipyridyl-4-yl]ethane] (8.2 mmol) and 900 mg of [Ru(4'-diethylphosphonate-2,2':6',2''-terpyridine)(Cl)₃] (1.56 mmol) in 100 mL of dimethylformamide. The mixture was brought to reflux under N₂, and within 15 min the solution was a deep crimson color. Refluxing was continued for 5 h, after which time all of the dimethylformamide was removed by rotary evaporation. The product mixture was redissolved in water and filtered to remove unreacted ligand. The pH of the aqueous solution was brought to 1 with concentrated hydrochloric acid, and then refluxed overnight to effect hydrolysis of the phosphonate ester groups, yielding [Ru^{II}(4'-phosphonic acid-2,2':6',2''-terpyridine)(1,2-bis[4'-methyl-2,2'-bipyridyl-4-yl]ethane)(Cl)]. The complex could be isolated from water as the zwitterionic "[Ru^{II}(4'-P(O)(OH)(O⁻)-2,2':6',2''-terpyridine)(1,2-bis[4'-methyl-2,2'-bipyridyl-4-yl]ethane)(Cl⁻)]" and was then

reacted overnight with 1.0 g of NaCN (20 mmol) in ~60 mL of refluxing dimethylformamide containing 20 mL of 0.1 M NaOH. After rotary evaporation of all solvent, the complex was redissolved in water and the pH lowered to ~2 by the addition of dilute trifluoromethanesulfonic acid. The precipitated product was collected by filtration and dried under vacuum.

[Ru^{II}(4'-phosphonic acid-2,2':6',2''-terpyridine)(4,4'-dimethyl-2,2'-bipyridine)(CN)] (Dye 2). This complex was prepared in identical fashion to dye 1, except that in the intermediate step to prepare [Ru(4-diethylphosphonate-2,2':6',2''-terpyridine)(4,4'-dimethyl-2,2'-bipyridine)(Cl)] 153.8 mg of [Ru(4'-diethylphosphonate-2,2':6',2''-terpyridine)(Cl)₃] (0.267 mmol) and 65.2 mg of 4,4'-dimethyl-2,2'-bipyridine (0.35 mmol) were used.

[Ru^{II}(4-phosphonic acid-2,2'-bipyridine)₂(1,2-bis[4'-methyl-2,2'-bipyridyl-4-yl]ethane)] (Dye 3). [Ru^{II}(4-diethyl phosphonate-2,2'-bipyridine)₂Cl₂] was prepared according to a literature preparation⁴⁷ using 483 mg of 4-diethyl phosphonate-2,2'-bipyridine (1.65 mmol), 216 mg of RuCl₃·3H₂O (0.825 mmol), and 233 mg of LiCl (5.5 mmol). The product was converted to [Ru^{II}(4-phosphonic acid-2,2'-bipyridine)₂Cl₂] by refluxing overnight in 0.5 M HCl. The product was refluxed in dimethylformamide containing 853 mg of 1,2-bis[4'-methyl-2,2'-bipyridyl-4-yl]ethane (2.3 mmol) for approximately 16 h. The dimethylformamide was rotary evaporated, and the reaction mixture was redissolved in water and filtered to remove excess ligand. The aqueous portion was rotary evaporated to dryness and then dried under vacuum.

[Ru^{II}(4,4'-bis(methylphosphonic acid)-2,2'-bipyridine)₂(4,4',5,5'-tetramethyl-2,2'-bipyridine)] (Dye 4). [Ru^{II}(4,4'-bis[diethyl methylphosphonate]-2,2'-bipyridine)₂Cl₂] was prepared via modification of a literature preparation,⁴⁷ using 305 mg of 4,4'-bis(diethyl methylphosphonate)-2,2'-bipyridine (0.669 mmol), 87.0 mg of RuCl₃·3H₂O (0.333 mmol), and 94 mg of LiCl (2.2 mmol). Subsequently, 100.3 mg of [Ru^{II}(4,4'-bis[diethyl methylphosphonate]-2,2'-bipyridine)₂Cl₂] (0.0925 mmol) and 39 mg of 4,4',5,5'-tetramethyl-2,2'-bipyridine (0.20 mmol) in 3 mL of dimethylformamide and 2 mL of 0.1 M KOH were refluxed for 6 h under an argon atmosphere. The reaction mixture was rotary evaporated to dryness, redissolved in water, and made neutral by the addition of dilute sulfuric acid. Excess, unreacted 4,4',5,5'-tetramethyl-2,2'-bipyridine was filtered from the aqueous solution; the pH was made to ~1 and the solution refluxed overnight to ensure hydrolysis of the phosphonate groups. All attempts to crash the complex out of aqueous solution via pH manipulation were unsuccessful. Instead, the pH was made neutral by addition of dilute NaOH and the solution rotary evaporated to dryness. Redissolution in ethanol allowed the filtering out of excess salts.

M-4,4',4'',4'''-tetracarboxyphthalocyanines (Dyes 5 and 6). Fe^{III}-4,4',4'',4'''-tetracarboxyphthalocyanine (dye 6) was prepared according to Shirai et al.⁴⁸ Mg^{II}-4,4',4'',4'''-tetracarboxyphthalocyanine (dye 5) was prepared similarly; however, magnesium acetate was used in place of the metal chloride. Purity of the phthalocyanines was assessed via absorption spectra and cyclic voltammetry.

3,4,9,10-Perylenedihydroxamic Acid Dianhydride (Dye 7). The dye was prepared by variation of the method employed by Ford to prepare the di(glycyl)imide derivative.⁴⁹ 3,4,9,10-Perylenetetracarboxylic acid dianhydride (260 mg, 0.663 mmol) was suspended in ~25 mL of dimethyl sulfoxide and heated to 90 °C. Hydroxylamine hydrochloride (1.1 g, 16 mmol) and KOH (900 mg, 16 mmol) dissolved in ~20 mL of water were subsequently added to the hot suspension. A condenser was

attached, and heating was continued for 3 h. The dark precipitate was collected on a 0.45 μm filter and then heated in 0.5 M HCl. The acidified precipitate was again collected and rinsed with water. The product was purified by recrystallization in methanol and dried under vacuum. Although the initial yield is high (>90%), due to its sparing solubility in methanol, yields after purification are much lower (~10%). Its identity was confirmed by absorption and infrared spectra.

[Ru^{II}(4,4'-dicarboxylic acid-2,2'-bipyridine)₂(4,4'-dimethyl-2,2'-bipyridine)] [PF₆]₂ (Dye 8). [Ru^{II}(4,4'-dicarboxylic acid-2,2'-bipyridine)₂Cl₂] was prepared according to Meyer⁴⁷ employing 913.3 mg of 4,4'-dicarboxylic acid-2,2'-bipyridine (3.740 mmol), 488.4 mg of RuCl₃·3H₂O (1.871 mmol), and 529 mg of LiCl (12.5 mmol). Next, 409 mg of [Ru^{II}(4,4'-dicarboxylic acid-2,2'-bipyridine)₂Cl₂] (0.62 mmol) was reacted with 136 mg of 4,4'-dimethyl-2,2'-bipyridine (0.739 mmol) in ~50 mL dimethylformamide containing 10 mL of 0.1 M NaOH. The solvent was rotary evaporated and the reaction mixture dissolved in water; the pH was made neutral by the addition of dilute trifluoromethanesulfonic acid, and excess ligand was filtered off. The pH was lowered further to pH 2; an aqueous, saturated solution of ammonium hexafluorophosphate was added. There was only partial precipitation of the complex as the PF₆⁻ salt; the precipitated portion was collected by vacuum filtration, rinsed with water, and dried under vacuum.

TiO₂ Electrodes. Conductive glass substrates (Libby Owens Ford, 10 Ω /square F-SnO₂) were cleaned by overnight immersion in a solution of KOH in 2-propanol, rinsed with deionized water, and dried in a nitrogen stream. The TiO₂ colloidal suspension (preparation reported elsewhere³⁵) was spread over the substrate with a glass rod using adhesive tape as spacers. The films were fired at 450 °C for 45 min in air, resulting in an almost transparent film. The films thickness was 4 μm in the chemical oxidation experiments and 1.5 μm in the electrochemical experiments. The dyes were adsorbed by immersing the electrodes overnight in a 0.5 mM aqueous or acetonitrile solution of the dye.

Measurements. Electrochemical measurements were performed with a PAR 173 potentiostat in a three-electrode arrangement. Potentials are reported vs SCE. Absorption spectra were measured with a HP 8453 spectrophotometer using an undyed nanocrystalline TiO₂ electrode as a reference. Fluorescence emission spectra were measured with an Aminco Bowman AB2 Spectrofluorometer employing a front face electrochemical cell. Both the spectro-electrochemical reduction and the potential-dependent photoluminescence experiments were done in dry conditions using a sealed cell that was loaded in a nitrogen atmosphere glovebox. The electrolyte solution was 0.1 M LiClO₄ or 0.1 M tetrabutylammonium hexafluorophosphate (TBAPF₆) in dry acetonitrile (Burdick & Jackson, distilled over calcium hydride). The reference electrode for these experiments was a silver wire calibrated vs ferrocene/ferrocenium and reported vs SCE.

The oxidation or reduction potentials of the different ruthenium-based dyes in solution were determined by cyclic voltammetry. The experiments used a platinum or glassy carbon working electrode, an SCE reference electrode, and a platinum counter electrode. In one case (dye 5) the oxidation potential was determined by spectrochemical titration. An I₂ oxidizing solution was added to the dye solution, and the fraction of oxidized dye was determined from the change in the solution absorption spectrum. A plot of the fraction of oxidized dye as a function of the solution potential yielded the oxidation potential.

The chemical oxidation experiments were carried out using an aqueous solution of either Br₂ or I₂ as the oxidizing solution. The concentration of the oxidizing species (Br₂ or I₂) in the solution was 10⁴ times higher than the amount of dye on the film, so the change in potential of the solution resulting from oxidation of the dye was negligible. The fraction of dye oxidized in each experiment was fitted to the potential of the specific oxidizing solution, measured both before and after the dye oxidation. A stock solution of 20 mM Br₂ or I₂ in HClO₄ was made at pH 2, and the pH was adjusted by addition of NaOH. The ionic strength was approximately constant throughout the pH range. Control experiments at higher ionic strengths up to 200 mM showed no change in the fraction of oxidized dye with increasing ionic strength.

Results and Discussion

Cyclic voltammetry was employed to measure the oxidation potentials of the different ruthenium dyes in solution as a function of solution pH (cyclic voltammograms of dye 1 were reported in ref 35). The oxidation potential of the phthalocyanine dye (dye 5) as a function of the solution pH was resolved by spectrochemical titration experiments (see Experimental Section). The formal potentials of the different dyes in solution are listed in Table 1. The electron-transfer processes in all cases are chemically reversible and the dyes are stable in both oxidation states. Over the pH range of our experiments (pH 2–8), the oxidation potentials of all dyes in solution were found to be independent of pH.

Once adsorbed to the nanocrystalline TiO₂ film, the dyes remained strongly bound in aqueous solutions below pH 8.5. Above this value they desorbed; thus, our experimental window was limited to values less than pH 8.5. The chemical oxidation experiments were carried out as described previously.³⁵ The overall procedure was employed for each dye using the oxidizing solution (Br₂ or I₂) that most closely matched the oxidation potential of the specific dye.

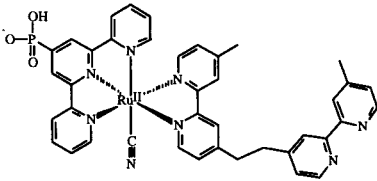
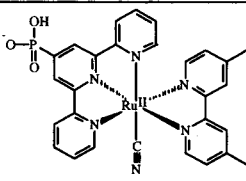
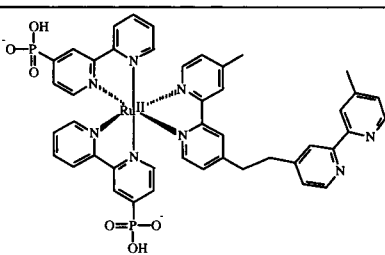
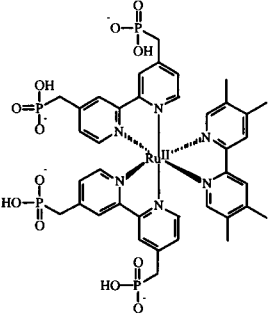
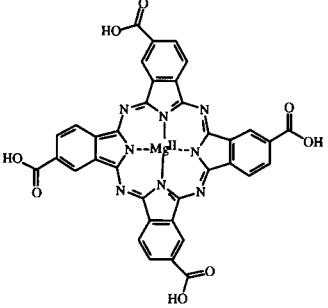
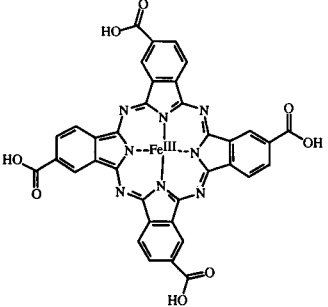
Figure 1 presents a set of absorption spectra of a dye-sensitized film at different degrees of oxidation. The films shown in Figure 1 were sensitized with phthalocyanine (dye 5), which serves as a typical example of the measurements and the calculations (a similar set of spectra with dye 1 can be found in ref 35). Curve a in Figure 1 shows the spectrum of the dye-sensitized film before oxidation. Curve b shows the absorbance of the film after immersion in aqueous I₂ solution at pH 2.8 for 10 min. By comparison with the original spectrum (curve a) and with the spectrum of the fully oxidized dye (curve d), it is apparent that the dye was partially oxidized at pH 2.8. Exposure of the partially oxidized film to triethylamine results in the re-reduction of the dye (curve c). The spectrum after re-reduction was almost the same as the original spectrum, showing that the dye neither desorbed nor decomposed during the experiment. The film could not be completely oxidized by I₂ solution in the available pH range. Therefore, the spectrum of the completely oxidized dye (curve d) was obtained by immersing the film in an aqueous solution of the stronger oxidant, Br₂.

The fraction, x , of the dye oxidized by the oxidizing solution at each pH was calculated from the absorption spectra as described previously.³⁵ The resulting values of x were employed to calculate the oxidation potential, $E^{0'}$, of the dye at each pH using the Nernst equation:⁵⁰

$$E^{0'} = E - (RT/nF) \ln[x/(1-x)] \quad (1)$$

where E is the potential of the oxidizing solution, R , T , and F

TABLE 1: pH-Dependent Redox Potential Induced in Sensitizing Dyes by Specific Adsorption onto Oxide Surfaces

Dye		Substrate	Sensitivity (mV / pH)	E^0 at pH=0 (mV) calc'd	E^0 in Sol. (mV)
Dye 1: [Ru ^{II} (4'-phosphonic acid-2,2':6',2''-terpyridine)(1,2-bis[4'-methyl-2,2'-bipyridyl-4-yl]ethane)(CN)]		TiO ₂	53.7 ± 4.6	1421 ± 30	990
		Al ₂ O ₃	53.6 ± 9.5	1393 ± 42	990
Dye 2: [Ru ^{II} (4'-phosphonic acid-2,2':6',2''-terpyridine)(4,4'-dimethyl-2,2'-bipyridine)(CN)]		TiO ₂	42.5 ± 2.1	1281 ± 16	930
Dye 3: [Ru ^{II} (4-phosphonic acid-2,2'-bipyridine) ₂ (1,2-bis[4'-methyl-2,2'-bipyridyl-4-yl]ethane)]		TiO ₂	51.4 ± 5.9	1389 ± 37	1000
Dye 4: [Ru ^{II} (4,4'-Bis(methylphosphonic acid)-2,2'-bipyridine) ₂ (4,4',5,5'-tetramethyl-2,2'-bipyridine)]		TiO ₂	29.7 ± 2.3	1211 ± 15	970
Dye 5: Mg ^{II} -4,4',4'',4'''-tetra-carboxyphthalocyanine		TiO ₂	20.6 ± 1.8	653 ± 13	570
Dye 6: Fe ^{III} -4,4',4'',4'''-tetra-carboxyphthalocyanine		TiO ₂	26.4 ± 3.4	736 ± 26	

are the Boltzmann constant, the temperature, and the Faraday constant, respectively, and n is the number of electrons involved

in the oxidation process. For all dyes a linear correlation between the oxidation potential of the adsorbed dye (E^0) and

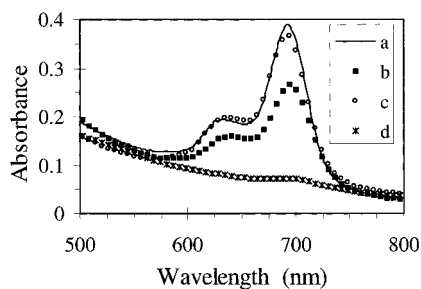


Figure 1. Typical absorption spectra of the adsorbed phthalocyanine dye 5: (a) initial spectrum before oxidation, (b) after partial oxidation with aqueous I_2 solution at pH 2.8, (c) after re-reduction of the dye with triethylamine, and (d) after complete oxidation with aqueous Br_2 solution.

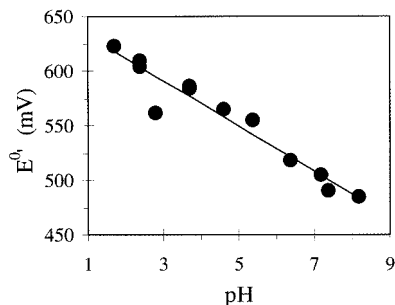


Figure 2. Formal potential ($E^{0'}$) of adsorbed dye 5 as a function of the pH of the iodine solution. The line is a linear fit showing 20.6 mV shift of $E^{0'}$ per pH unit. $E^{0'}$ was calculated from equation 1.

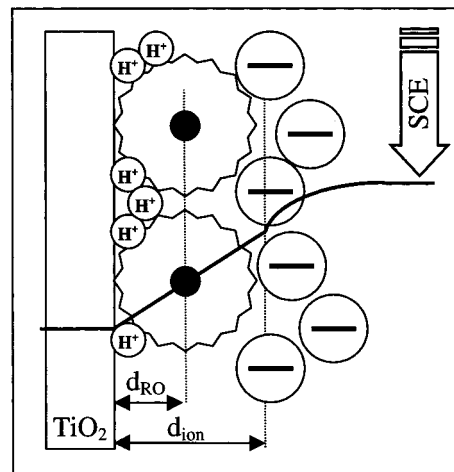
the pH of the oxidizing solution was found. In Figure 2, for example, the oxidation potential of dye 5 when adsorbed onto TiO_2 is plotted as a function of the pH of the oxidizing solution. As the pH increases, $E^{0'}$ decreases by 20.6 ± 1.8 mV per pH unit, in contrast to the pH-independent oxidation potential when dye 5 is dissolved in solution. The linear correlation between $E^{0'}$ of the adsorbed dye 5 and the pH predicts that at pH 0 the oxidation potential will be shifted 83 ± 13 mV positive of its solution value. The corresponding values for all dyes studied (dyes 1 through 6) are presented in Table 1. The oxidation potentials of all six dyes became pH-sensitive upon adsorption onto TiO_2 , the dependence varying between 21 and 53 mV per pH unit.

In a previous paper,³⁵ we proposed two possible mechanisms for the induced pH dependence. Both mechanisms suggested that the induced pH dependence was related to the well-known 59 mV per unit pH shift of the flat band potential of oxide semiconductors.^{36,37} The flat band potential shift was proposed to affect the adsorbed dye (i) by the strong electronic interaction between the dye and the TiO_2 that is necessary to achieve the high quantum efficiencies (>80%) for electron injection observed in these systems or (ii) by the influence of the electrostatic field caused by the adsorption of ions (H^+ and OH^-) on the semiconductor surface.

Chemical oxidation experiments on dye 1 adsorbed onto high surface area aluminum oxide films were performed in order to check the validity of the first mechanism. Insulating aluminum oxide was chosen to exclude the possibility of electronic interactions between the dye and the substrate. The conduction band of Al_2O_3 is much too far negative to interact with the dye. The pH dependence of dye 1 on Al_2O_3 was identical to that on TiO_2 (Table 1). These results clearly indicate that electronic interactions between the dye and the oxide surface are not necessary to induce the pH dependence.

The second mechanism, on the other hand, is consistent with the results reported in Table 1. The influence of an electric

SCHEME 1: Simplified Schematic View of the Dye-Coated TiO_2 -Solution Interface^a



^a As shown, protons can penetrate the dye monolayer, generating a pH-dependent potential difference between the oxide surface and a reference electrode in solution, but the much larger anions are largely constrained to reside outside the dye layer. Therefore, a fraction of the pH-dependent potential difference must drop across the dye, affecting its apparent redox potential. The magnitude of this effect depends on the ratio between d_{RO} , the distance between the oxide surface and the redox-active part of the dye (the ruthenium atom for oxidation of the ruthenium dyes), and d_{ion} , the average distance of closest approach of the centers of the anions.

field on an adsorbed monolayer of molecules containing reversible redox centers has been studied in the context of chemical modification of electrodes,^{51,52} and as a result, models that describe the voltammetric response and electron transfer kinetics at such electrodes were developed.^{53,54} These studies show that when electrolyte ions are constrained to remain on the solution side of the adsorbed layer, part of the potential difference between the electrode and the solution drops across this layer, thus affecting the apparent potential of the embedded redox centers. The dye-coated TiO_2 films also consist of large specifically adsorbed species (dye) containing redox centers. The models developed previously can therefore be used to describe, at least qualitatively, the processes at the dye-coated TiO_2 electrode/solution interface.

Scheme 1 presents a schematic view of the dye-coated TiO_2 /solution interface. The arguments presented here are equally valid for other oxide surfaces. The dye monolayer cannot sterically block the adsorption of the small H^+ or OH^- ions on the TiO_2 surface; however, it does control the average distance of nearest approach of the centers of the large negative counterions (d_{ion}). As a result, the potential of the TiO_2 bands shift by 59 mV/unit pH versus a reference in solution, and a fraction of this potential difference drops across the dye layer. Being inside the pH-dependent electric field, the redox center of the dye is affected so that its measured potential also shifts with pH. Note that this effect does not require the existence of a compact monolayer but only that some fraction of the pH-induced electric field drops across the dye, that is, that the dye is at least partially inside the ionic double layer at the substrate/solution interface.

The location of the dye redox center with respect to the ionic double layer is determined by the ratio between d_{RO} , the distance between the TiO_2 and the redox centers, and d_{ion} . In the simple case of a linear potential drop across the adsorbed dye layer, the fraction of the potential drop that affects the dye can be approximately expressed as $S_{pH} = 1 - (d_{RO}/d_{ion})$, defined as

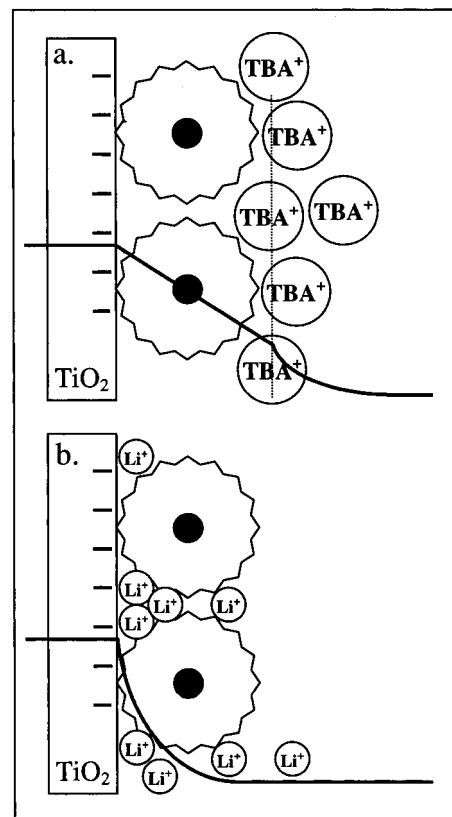
the sensitivity. The maximum potential shift of 59 mV/unit pH occurs when $S_{\text{pH}} = 1$ and may approach zero when $S_{\text{pH}} = 0$. High S means that the redox potential of the dye closely follows the flat band potential of the semiconductor, while low S means it is almost independent of changes in the semiconductor potential. The exact electric field distribution at this interface depends on a number of factors such as the dielectric properties of the solution and the dye, the geometry of the surface, the dye coverage, the identity and concentration of the electrolyte ions, etc. The potential drop across the dye layer is not necessarily linear, and the linear illustration in Scheme 1 is just the simplest case. Qualitatively, however, S_{pH} will be employed below to explain the variation in pH dependence between the different dyes.

According to the proposed model (Scheme 1), the sensitivity of the dye redox potential to pH-induced changes in the semiconductor potential depends on the molecular structure of the dye, other factors being constant. To check the validity of the model, the sensitivities of dye 1 and dye 2, that differ only by the additional outboard bipyridine linked to dye 1 (Table 1), were measured. The distances between the redox center of these dyes (the ruthenium atom in the case of oxidation of Ru^{II} to Ru^{III}) and the TiO₂ (d_{RO}) should be similar, as both dyes adsorb to the TiO₂ through their phosphonic acid group. However, d_{ion} of dye 1 is expected to be larger than d_{ion} of dye 2, because of the additional bipyridine. Therefore, the S_{pH} value ($1 - d_{\text{RO}}/d_{\text{ion}}$) of dye 1 should be larger than the S_{pH} value of dye 2. The measured sensitivity to pH of dye 1 (54 mV/pH, Table 1) is, in fact, higher than the measured sensitivity of dye 2 (43 mV/pH), in agreement with the proposed model.

Precise simulation of the potential distribution across the dye layer and accurate calculations of either d_{RO} or d_{ion} are beyond the scope of this work. But a qualitative discussion of the pH sensitivities of the various dyes is possible. The reason that dye 1 has a higher S_{pH} value than dye 2 was just discussed. Both dye 3 and dye 1 show a large pH dependence, probably due to the size of the external bipyridine ligand that increases the nearest approach distance of the negative ions (d_{ion}). The lower sensitivity of dye 4 compared to dye 2 may result from the following: the additional methyl on the phosphonic acid bonding group of dye 4 that decreases S_{pH} , the different bonding of dye 4 to the TiO₂ (through 2 to 3 bonding groups), or the effect of the unbound, ionizable phosphonic acid group on the potential distribution across the dye layer. The adsorbed phthalocyanine dyes (dyes 5 and 6) have the smallest induced pH dependence. These dyes probably adhere to the TiO₂ through all four carboxylic acid groups in a flat configuration. Their redox center is delocalized over the whole molecule rather than being localized on a specific atom. The small sensitivity to the pH-induced band edge movement measured for these dyes may indicate that d_{RO} and d_{ion} of the phthalocyanine dyes are almost the same.

Additional support for the proposed description of the dye-coated TiO₂/solution interface is provided by spectro-electrochemical reduction and potential-dependent photoluminescence experiments. In addition, these experiments provide insight into the processes occurring in dye-sensitized systems in nonaqueous solution during actual cell operation. Scheme 2 presents a schematic view of the dye-coated TiO₂-solution interface as negative bias is applied to the TiO₂ electrode in the dark. When the positive ions in solution are large, such as tetrabutylammonium (TBA⁺), they cannot penetrate the dye layer and thus part of the potential difference between the TiO₂ and the solution drops across the dye layer (Scheme 2a). Apart from the different

SCHEME 2: Schematic View of the Dye-Coated TiO₂-Solution Interface As Negative Bias Is Applied to the TiO₂ Electrode in the Dark^a



^a As shown, the electric field at this interface depends on the size of the electrolyte ions. The position of the specifically adsorbed dye relative to the ionic double layer determines whether the dye is strongly affected by the applied potential (a) or not (b).

origins for the potential difference across the dye layer, Schemes 1 and 2a represent the same processes. Therefore, employing the same arguments that were used for the pH-dependent case, the following observations are expected: The apparent redox potential of the dye will depend on the applied bias, that is, the dye, to some extent, will follow the potential of the semiconductor, but the potential of the dye will change by only part of the applied potential difference because the redox center is positioned at some distance from the TiO₂ ($S_{\text{pH}} < 1$). In contrast, when the positive ions in solution are small, such as Li⁺, the ions may penetrate the dye layer and the applied potential will decay nonlinearly over a very short range (Scheme 2b). In this case the redox centers may be located primarily outside the electric field; therefore, the redox potential of the dye should show only a weak dependence on the potential applied to the semiconductor.

Both the spectro-electrochemical reduction and the potential-dependent photoluminescence experiments examine the redox potential of a dye during a bias sweep as a function of the size of the cations (TBA⁺ or Li⁺). The experiments were carried out in dry conditions to ensure that only the desired ions are present (elimination of protons in particular). It is also important to note that thin (1.5 μm) TiO₂ films were used in these experiments, because ion motion through the porous films will neutralize the applied potential over a short distance.⁶

The spectro-electrochemical reduction experiments were done using the perylene dye shown in Figure 3 (dye 7). This dye was chosen because its reduction occurs at a potential more positive than the potential at which it desorbs from the TiO₂.⁶

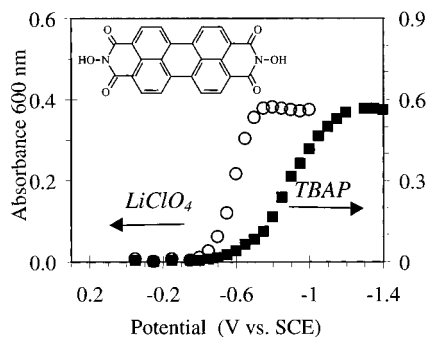


Figure 3. Absorbance at 600 nm of perylene dye 7 (shown as inset) adsorbed to porous TiO_2 as a function of the applied potential. The dye reduction process, evidenced by the 600 nm peak growth, shows a marked dependence on the type of ion used.

In solution, the first reduction potential of this dye was measured to be -0.61 V vs SCE. The reduction results in the decrease of the original absorption peak at 495 nm and the appearance of a new absorption peak at 600 nm allowing the process to be monitored spectrally. The spectro-electrochemical reduction experiments were done as follows: absorption spectra of the dye-coated film, compared to an uncoated film as baseline, were measured during a 1 mV/s potential sweep, and the absorption at 600 nm was plotted as a function of the applied bias. This procedure was repeated with both TBA^+ - and Li^+ -containing solutions.

The absorbance at 600 nm of two films is shown in Figure 3 as a function of the applied potential. The dye reduction process, evidenced by the 600 nm peak growth, shows a marked dependence on the type of ion used. Two parameters reflect this dependence: the voltage at which half of the dye is reduced ($x = 1/2$), $E_{1/2}$, and the deviation from the Boltzmann distribution of an order of magnitude change in x every 59 mV. In the Li^+ solution the reduction potential of the adsorbed dye was -0.60 V, the same as in solution, and x was calculated to change by 97 mV/decade. The small deviation from the Boltzmann distribution is probably caused by the gradient of potential through the porous electrode.⁶ In contrast, when the film was immersed in TBA^+ solution, $E_{1/2}$ shifted to -0.89 V and a large deviation from the Boltzmann distribution, 227 mV/decade, was observed. These results are consistent with those expected from the model shown in Scheme 2.

Similar behavior was measured in the potential-dependent photoluminescence experiments. These experiments measure the ability of the excited state of the dye to inject electrons into the TiO_2 as a function of the TiO_2 potential. Since efficient injection occurs only when the potential of the TiO_2 conduction band is positive of the excited-state oxidation potential of the dye,²⁹ it is possible to stop the injection process with an externally applied negative bias. Figure 4 presents the normalized photoemission of two TiO_2 films coated with dye 8 (shown as an inset in Figure 4) as a function of the external bias and the type of electrolyte solution. The emission is normalized to represent the ratio between the intensity during the potential sweep and the intensity at 0.15 V. As the potential is scanned negatively the emission intensity increases, indicating that the injection rate is becoming slower relative to the rate of luminescence. The changes in emission intensity with potential are completely reversible. The onset potential of the emission increase, when the film is immersed in the TBA^+ solution, is approximately 400 mV negative of the onset potential in the Li^+ solution. In other words, there is a potential range at which the injection rate is slowed down in the presence of Li^+ but is unaffected in the TBA^+ solution. These results lend further

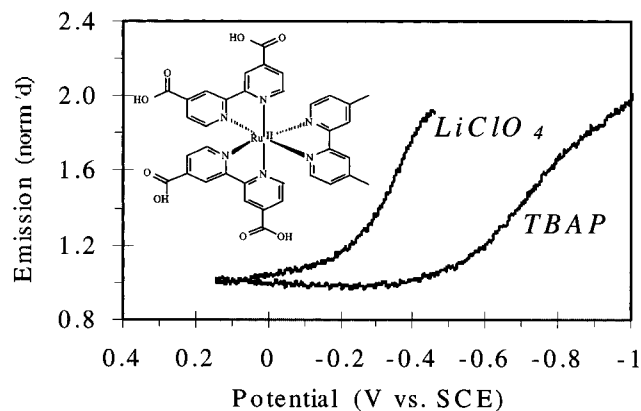


Figure 4. Normalized photoluminescence of dye 8 (shown as inset) adsorbed to porous TiO_2 as a function of the external bias and the type of electrolyte solution. The decreased rate of electron injection with negative bias, evidenced by the increased photoemission, shows a marked dependence on the type of ion used. The emission is normalized to represent the ratio between the intensity during the potential sweep and the intensity at 0.15 V.

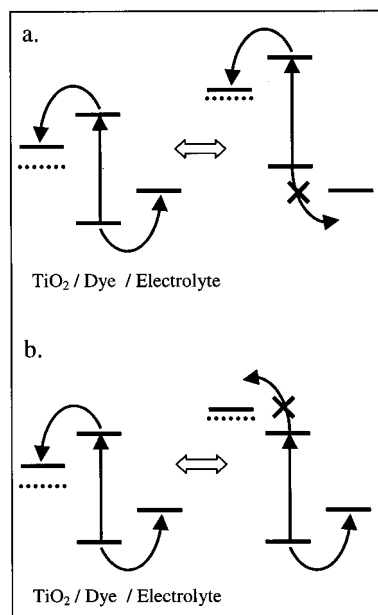
support to the conclusion that, in the presence of the small Li^+ ions, the dye potential is only weakly dependent on the potential of the TiO_2 , while in the presence of the large TBA^+ ions, it shifts by a substantial fraction of the applied potential. Both the spectro-electrochemical reduction and the potential-dependent photoluminescence experiments support the description of the dye-coated TiO_2 -solution interface presented in Scheme 2.

It is important to note that the energetics of the adsorbed dye become sensitive to either the pH or the external bias, that is, to potential changes of the semiconductor, when the redox center of the dye is located inside the ionic double layer. This condition is not met in a system that contains either small ions or weakly (nonspecifically) bound dyes. In both cases the counterions will be able to neutralize much of the electric field over a range that is shorter than the distance between the substrate and the redox center of the dye. Indeed, Sonntag and Spittler⁵⁵ showed that a weakly adsorbed carbocyanine-type sensitizing dye exhibited a clear pH threshold for electron injection into single-crystal SrTiO_3 . In this case, the potential of the dye was not affected by changes in the flat band potential of the semiconductor.

The results presented in this paper show that the dye potential is not fixed relative to either the semiconductor or the solution potential. Two processes that may cause a shift in the semiconductor potential occur in a dye-sensitized cell under working conditions: (1) electrostatic charging of the semiconductor by external bias or by photoinjection of electrons from dyes and (2) adsorption of solution components (such as *tert*-butylpyridine and chenodeoxycholic acid that are often used as electrolyte additives) to the oxide surface. The potential of the dye may or may not follow the shift in the semiconductor potential depending on the factors discussed above.

The possible shift in dye potential in a working cell should be accounted for when these cells are being investigated or designed. For example, Scheme 3 illustrates two (of many) cases depicting possible kinetic limitations to the cell's open-circuit photovoltage: one limited by the dye regeneration process (a) and the other by the dye electron injection process (b). When the dye potential closely follows the potential of the TiO_2 (Schemes 2a and 3a), negative applied or photogenerated bias should not markedly change the electron injection rate but could substantially slow the dye regeneration process

SCHEME 3: Simplified Energy Diagram of the Semiconductor/Dye/Electrolyte Interface in a Working Dye-Sensitized Cell^a



^a The diagrams on the left illustrate the energetics at short circuit, while the diagrams on the right indicate two of the possible kinetic limitations to the open-circuit photovoltage, V_{oc} . (a) When the dye potential approximately follows the semiconductor potential (conditions of Scheme 2a), V_{oc} could be limited by the decreasing rate of oxidized dye regeneration by solution species. (b) When the dye potential is approximately independent of the semiconductor potential (conditions of Scheme 2b), V_{oc} could be limited by the decreasing rate of photoinjection into the semiconductor. There are many other possible kinetic limitations to V_{oc} .

as the ground-state oxidation potential of the dye becomes more negative than the solution potential. On the other hand, if the dye potential is almost fixed relative to the solution (Schemes 2b and 3b), a negative shift in TiO₂ potential should not slow the regeneration rate but may substantially slow the injection rate. Other limitations of the open-circuit photovoltage are also possible, but whether the dye moves with the TiO₂ potential or not is clearly an important factor to be considered when attempting to understand or control the open-circuit voltage.

Most of the currently reported dye-sensitized solar cells consist of liquid electrolytes containing small positive and negative ions (Li⁺, I⁻, and I₃⁻). In these systems only small potential shifts of the dye relative to solution, but large shifts relative to the semiconductor, may be anticipated. In fundamental investigations, however, large potential shifts may occur relative to solution when large counterions are used. Large shifts in the dye potential may also occur in solid-state versions of the dye-sensitized cell.

In an earlier paper⁶ we reported that electric fields in porous TiO₂ electrodes are neutralized over a short range due to ion motion through the pores of the TiO₂. As a result, a gradient of potential is created both across the porous TiO₂ and in the electrolyte solution that penetrates the pores. In the current paper, changes in the relative potentials at the TiO₂/dye/electrolyte interface were revealed. When both studies are taken into account, the following picture emerges: during photovoltaic operation, the potentials of the TiO₂, the solution, and the dye may all vary with distance from the substrate electrode and may vary with respect to each other. That is, the local potential of all three components of the system may vary in a complicated way throughout the film. This suggests that theoretical modeling

of these systems may be very difficult. In any case, the usual models borrowed from standard semiconductor physics are not applicable to these electrodes.

Conclusion

The effect of specific adsorption to oxide surfaces on the redox potential of sensitizing dyes was studied. The investigated dyes exhibited adsorption-induced pH-dependent redox potentials that varied between 21 and 53 mV per pH unit depending on the dye structure. The redox potential of the dye was also affected by externally applied biases. The magnitude of these effects depended on the ability of the electrolyte ions to penetrate the dye layer as well as on the dye structure. When the sensitizing dye is primarily inside the ionic double layer at the semiconductor oxide/solution interface, its redox potential will tend to follow the changes in the semiconductor potential. When the dye is primarily outside the double layer, its potential will be almost independent of the semiconductor potential. The fact that the potential of the dye is not fixed relative to either the semiconductor or the electrolyte solution has important implications for the understanding and optimization of dye-sensitized solar cells.

Acknowledgment. We are grateful to the U.S. Department of Energy for funding this research. A.Z. was supported by the Office of Energy Efficiency and Renewable Energy, Office of Utility Technologies, Photovoltaics Division; S.F. was supported by the Office of Energy Research, Office of Computational and Technology Research, Advanced Energy Projects Division; and B.A.G. was supported by the Office of Energy Research, Division of Basic Energy Sciences, Chemical Sciences Division.

References and Notes

- (1) Gerfin, T.; Grätzel, M.; Walder, L. In *Molecular Level Artificial Photosynthetic Materials*; Karlin, K. D., Ed.; John Wiley & Sons, Inc.: New York, 1997; pp 345–393.
- (2) O'Regan, B.; Grätzel, M. *Nature* **1991**, *353*, 737–740.
- (3) Nazeeruddin, M. K.; Kay, A.; Rodicio, I.; Humphry-Baker, R.; Muller, E. L.; P.; Vlachopoulos, N.; Grätzel, M. *J. Am. Chem. Soc.* **1993**, *115*, 6382–6390.
- (4) Bechinger, C.; Ferrere, S.; Zaban, A.; Sprague, J.; Gregg, B. A. *Nature* **1996**, *383*, 608–610.
- (5) Athanassov, Y.; Rotzinger, F. P.; Pechy, P.; Grätzel, M. *J. Phys. Chem. B* **1997**, *101*, 2558.
- (6) Zaban, A.; Meier, A.; Gregg, B. A. *J. Phys. Chem. B*, in press.
- (7) Lindstrom, H.; Rensmo, H.; Södergren, S.; Solbrand, A.; Lindquist, S. E. *J. Phys. Chem.* **1996**, *100*, 3084.
- (8) Cao, F.; Oskam, G.; Meyer, G. J.; Seanson, P. C. *J. Phys. Chem.* **1996**, *100*, 17021.
- (9) Konenkamp, R.; Wahi, A.; Hoyer, P. *Thin Solid Films* **1994**, *246*, 13.
- (10) Boschloo, G. K.; Goossens, A.; Schoonman, J. *J. Electroanal. Chem.* **1997**, *428*, 25.
- (11) Bedja, I.; Kamat, P. V.; Hua, X.; Lappin, A. G.; Hotchandani, S. *Langmuir* **1997**, *13*, 2398.
- (12) Bedja, I.; Hotchandani, S.; Kamat, P. V. *J. Phys. Chem.* **1994**, *98*, 4133–4140.
- (13) Ferrere, S.; Zaban, A.; Gregg, B. A. *J. Phys. Chem. B* **1997**, *101*, 4490–4493.
- (14) Kay, A.; Grätzel, M. *J. Phys. Chem.* **1993**, *97*, 6272–6277.
- (15) Kohle, O.; Ruile, S.; Grätzel, M. *Inorg. Chem.* **1996**, *35*, 4779.
- (16) Vogel, R.; Pohl, K.; Weller, H. *Chem. Phys. Lett.* **1990**, *174*, 241.
- (17) Hagfeldt, A.; Didriksson, B.; Palmqvist, T.; Lindstrom, H.; Södergren, S.; Rensmo, H.; Lindquist, S. E. *Sol. Energy Mater. Sol. Cells* **1994**, *31*, 481.
- (18) O'Regan, B.; Schwartz, D. T. *J. Appl. Phys.* **1996**, *80*, 4749.
- (19) Cao, F.; Oskam, G.; Seanson, P. C. *J. Phys. Chem.* **1995**, *99*, 17071.
- (20) Tennakone, K.; Kumara, G. R. A.; Kumarasinghe, A. R.; Wijayantha, K. G. U.; Sirimanne, P. M. *Semicond. Sci. Technol.* **1995**, *10*, 1689.
- (21) Murakoshi, K.; Kogure, R.; Yanagida, S. *Chem. Lett.* **1997**, *5*, 471.
- (22) Hagfeldt, A.; Grätzel, M. *Chem. Rev.* **1995**, *95*, 49–68.

- (23) Burfeint, B.; Hannappel, T.; Storck, W.; Willig, F. *J. Phys. Chem.* **1996**, *100*, 16463–16465.
- (24) Rabani, J.; Ushida, K.; Koichi, Y.; Stark, J.; Gershuni, S.; Kira, A. *J. Phys. Chem. B* **1997**, *101*, 3136.
- (25) Argazzi, R.; Bignozzi, C. A.; Heimer, T. A.; Meyer, G. J. *Inorg. Chem.* **1997**, *36*, 2–3.
- (26) Murakoshi, K.; Kano, G.; Wada, Y.; Yanagida, S.; Miyazaki, H.; Matsumoto, M.; Murasawa, S. *J. Electroanal. Chem.* **1995**, *396*, 27–34.
- (27) Heimer, T. A.; D'Arcangelis, S. T.; Farzad, F.; Stipkala, J. M.; Meyer, G. J. *Inorg. Chem.* **1996**, *35*, 5319.
- (28) Huang, S. Y.; Schlichthörl, G.; Nozik, A. J.; Grätzel, M.; Frank, A. J. *J. Phys. Chem. B* **1997**, *101*, 2576–2582.
- (29) Parkinson, B. A.; Spitzer, M. T. *Electrochim. Acta.* **1992**, *37*, 943.
- (30) Södergren, S.; Hagfeldt, A.; Olsson, J.; Lindquist, S. E. *J. Phys. Chem.* **1994**, *98*, 5552.
- (31) Fitzmaurice, D. *Sol. Energy Mater. Sol. Cells* **1994**, *32*, 289.
- (32) Lyon, L. A.; Hupp, J. T. *J. Phys. Chem.* **1995**, *99*, 15718.
- (33) Elliott, C. M.; Hershenhart, E. J. *J. Am. Chem. Soc.* **1982**, *104*, 7519.
- (34) Cao, F.; Oskam, G.; Searson, P. C.; Stipkala, J. M.; Heimer, T. A.; Farzad, F.; Meyer, G. J. *J. Phys. Chem.* **1995**, *99*, 11974.
- (35) Zaban, A.; Ferrere, S.; Sprague, J.; Gregg, B. A. *J. Phys. Chem.* **1997**, *101*, 55–57.
- (36) Nozik, A. J. *Annu. Rev. Phys. Chem.* **1978**, *29*, 189–222.
- (37) Gerischer, H. *Electrochim. Acta* **1989**, *34*, 1005.
- (38) Elliott, C. M.; Freitag, R. A.; Blaney, D. D. *J. Am. Chem. Soc.* **1985**, *107*, 4647–4655.
- (39) Gould, S.; Strouse, G.; Meyer, T. J.; Sullivan, B. P. *Inorg. Chem.* **1991**, *30*, 2942–2949.
- (40) Jones, R. A.; Roney, B. D.; Sasse, W. H. F.; Wade, K. O. *J. Chem. Soc. B* **1967**, 106–111.
- (41) Yan, S. G.; Hupp, J. T. *J. Phys. Chem.* **1996**, *100*, 6867–6870.
- (42) Hirao, T.; Masunaga, T.; Ohshiro, Y.; Agawa, T. *Synthesis* **1981**, *1*, 56–57.
- (43) Sasse, W. H. F.; Whittle, C. P. *J. Am. Chem. Soc.* **1961**, *83*, 1347.
- (44) Péchy, P.; Rotzinger, F. P.; Nazeeruddin, M. K.; Kohle, O.; Zakeeruddin, S. M.; Humphry-Baker, R.; Grätzel, M. *J. Chem. Soc., Chem. Commun.* **1995**, 65–66.
- (45) Constable, E. C.; Ward, M. D. *J. Chem. Soc., Dalton Trans.* **1990**, 1405.
- (46) Sullivan, B. P.; Calvert, J. M.; Meyer, T. J. *Inorg. Chem.* **1980**, *19*, 1404–1407.
- (47) Sullivan, B. P.; Salmon, D. J.; Meyer, T. J. *Inorg. Chem.* **1978**, *17*, 3334–3341.
- (48) Shirai, H.; Yagi, S.; Suzuki, A.; Hojo, N. *Makromol. Chem.* **1977**, *178*, 1889–1895.
- (49) Ford, W. E. *J. Photochem.* **1987**, *37*, 189–204.
- (50) Bard, A. J.; Faulkner, L. R. *Electrochemical Methods Fundamental and Applications*; John Wiley & Sons: New York, 1980.
- (51) Chidsey, C. E. D. *Science* **1991**, *251*, 919.
- (52) Finklea, H. O.; Hanshew, D. D. *J. Am. Chem. Soc.* **1992**, *114*, 3173.
- (53) Smith, C. P.; White, H. S. *Anal. Chem.* **1992**, *64*, 2398–2405.
- (54) Creager, S. E.; Weber, K. *Langmuir* **1993**, *9*, 844–850.
- (55) Sonntag, L. R.; Spitzer, M. T. *J. Phys. Chem.* **1985**, *89*, 1453.